15

MR-Based Methods for pH Measurement in Brain Tumors: Current Status and Clinical Potential

Xiao-Fang Cheng[1] and Ren-Hua Wu[1,2]
[1]*Department of Medical Imaging, the 2nd Affiliated Hospital, Shantou University Medical College, Shantou,*
[2]*Provincial Key Laboratory of Medical Molecular Imaging, Guangdong Province, China*

1. Introduction

This study is supported in part by a grant from the National Natural Science Foundation of China (NSFC), key program 30930027. Corresponding to Wu RH.
Alteration in tissue pH is an indicator of many pathological processes. In tumors, the pH gradient exists between the intracellular (pHi) and extracellular (pHe) compartments. pHe is usually lower, and pHi could be higher or unchanging compared with normal tissue, which can be correlated with prognosis and response to treatment. In recent years, non-invasive MR-based methods have been developed to assess tissue pH in brain tumors. In addition to protons (^{1}H) and phosphorus (^{31}P), pH measurement approaches have been applied with other NMR nuclei such as fluorine (^{19}F) and carbon (^{13}C). By using hyperpolarized ^{13}C-labelled bicarbonate, the average tumor interstitial pH was found significantly lower than the surrounding tissue in mouse tumor model. Gd (3+)-based pH sensors and chemical exchange-dependent saturation transfer （CEST） and paramagnetic (PARACEST) agents are useful for further delineation of brain tumors. We use an optimized CEST technique to provide non-invasive pH information for human brain tumors. This article primarily focuses on the measurement of pH in brain tumors with MR-based methods and relevant clinical potential.

2. pH and tumours

As we know, intra- and extracellular pH are regulated in a dynamic steady state driven by metabolic acid production, export of H^+ from cells, and diffusion of these H^+ equivalents from the site of production to the blood, where they are buffered by an open and dynamic CO_2/HCO_3^- system[1]. However, although this balance is quite robust, many pathological states are associated with changes in tissue acid–base balance, including inflammation, ischaemia, renal disease, chronic lung disorders and intrauterine abnormalities [2-4] and tumors. In this review, we will focus on discussing pH alteration relevant to tumors.
Evidence accumulated over the past 50 years and more has shown that electrode-evaluated human tumor pH is on average, lower than the pH of normal tissues [5-6]. The increase in

hydrogen ion concentration is thought to be due to a combination of a more glycolytic phenotype, as well as reduced oxygen availability, leading to lactic acidosis from glycolysis [7].In addition, a poor and chaotic tumor vascularization leads to the inefficient washout of the acidic products and contributes further to development of the chronically acidic extracellular environment [8]. However, although most tumors had relatively acidic extracellular pH, there were some exceptions. Engin et al reported that tumour pHe was significantly different between different histological groups, the mean tumour pHe for the entire group of tumours was 7.06 +/- 0.05 (range 5.66-7.78) [9]. Prior to the application of ^{31}P-MRS to living tissue, it was not recognized that tissue pH is compartmentalized into an intracellular component (pHi) and an interstitial or extracellular component (pHe) [10]. To our knowledge, currently, there weren't concomitant measurements of pHi and pHe in spontaneous tumors. pH evaluated by electrodes primarily measures interstitial or extracellular tissue pH, whereas pH evaluated by^{31}P-MRS primarily reflects the aggregate pHi of tissue. pHi is similar in tumors and normal tissue. To date, the majority of pHi values have been obtained using ^{31}P-MRS. The measurement of pH by MRS is largely standardized, provides accuracy of±0.1 pH units [11]. The explaination is that the excess hydrogen ion is excreted from the cell by hydrogen ion pumps, in this way the intracellular environment is maintained at a more physiologically normal pH [5,12-13].

In recent years, there were some reports suggested that cellular uptake of chemotherapeutic drugs may depend on the pH gradient (pHi-pHe).The naturally occurring cell pH gradient difference between tumor and normal tissue is a major and exploitable determinant of the uptake of weak acids in the complex tumor microenvironment [14]. A low pHe enhances the uptake of weakly acidic drugs such as chlorambucil and 5-fluorouracil, whereas a low pHe reduces the uptake of mitoxantrone and the cytotoxicity of weakly basic drugs, such as doxorubicin [15-17]. By i.v.-injected glucose in a xenografted human tumor, Kozin [14] et al showed that the tumor-specific pH gradient may be exploited for the treatment of cancer by weak acid chemotherapeutics. Similarly, some efforts have been made to increase the intracellular acidity via disturbing the pH-regulating mechanisms, which therefore causing cell death at a sufficiently low pH [18-19]. To date, the majority of treatment-related studies conducted have focused on hyperthermia (combined with radiotherapy) due to the recognized importance of acidic pH as a thermal sensitizer. What surprised us for the results was that patients with a better response to hyperthermia radiotherapy have higher pH (as measured by electrode or ^{31}P MRS) prior to treatment [20].

3. pH measurement with ^{1}H-MRSI

With high inherent sensitivity of ^{1}H nucleus, many attempts have been made to produce pH-sensitive MRI contrast. Gillies et al[1] have employed an exogenously administered imidazole, IEPA, which has a pH-dependent chemical shift of the H-2 resonance in the 7-9 ppm range. This has been used for imaging pHe in orthotopic breast cancer by MR spectroscopic imaging (MRSI). Our colleagues [22] used conventional FSE sequence to study phantom (Histidine is included) and found there were some relationship between pH value and signal intensity on T2-weighted images, which enables the magnetic resonance pH imaging.

Currently, there were two major approaches for measuring pH, relaxation methods and magnetization transfer methods. Relaxation methods requires the injection of exogenous

contrast agents (CAs). Actually, magnetic resonance spectroscopy with ^{31}P or ^{19}F probes can be attached to a contrast agent (CA). Nevertheless, although these probes can be effective, ^{1}H-based probes are preferred because they are intrinsically the most sensitive of MR-based probes. Current clinical CAs are small-molecule Gd3+ chelates that work by shortening the longitudinal and/or transverse relaxation times of the protons in their close proximity. These relaxation agents have a number of shortcomings. First, they do not target specific areas or disease regions, nor do they respond to cellular stimuli, but rather they matriculate throughout the body, confined to the circulatory system, prior to eventual elimination [23]. As a consequence, relatively large agent doses are required to reach clear contrast detection. Second, patients suffered gadolinium exposure have risk in with renal insufficiency [24]. The rapidly emerging field of molecular imaging seeks to develop CAs as molecular probes that respond to cellular processes or cellular markers in contrary [23]. To date, some recent prototype MRI CAs that respond to pH have been developed [25-28]. Gadolinium-based carbon nanostructures were poised to make a significant impact as advanced CAs for magnetic resonance imaging (MRI) in medicine. It was forecasted that gadonanotubes as synthons for the design of high-performance MRI CA probe with efficacies up to 100 times greater than current clinical CAs. These new materials will be useful for in vivo MRI applications as circulating drug nanocapsules because of their low toxicities, extremely high relaxivities, and potential for cellular targeting and induced cell death by magnetic hyperthermia [29]. In Hartman's [23] study, gadonanotubes have also been shown to maintain their integrity when challenged ex vivo by phosphate-buffered saline solution, serum, heat, and pH cycling. Nevertheless, although these relaxation-based agents are responsive to the state of their environment (e.g. pH, temperature, etc.), the measured effect is a function of both the environment and the agent concentration, which is usually unknown in vivo, leading to the difficulty of quantification of the environmental parameter of interest [30]. In addition, only one target per MRI exam can be obtained with targeted relaxation contrast agents [31]. Considering the limitations of relaxation-based agents mentioned above, a new class of contrast agents is required. It was reported that use of chemical-exchange-dependent saturation transfer (CEST) methods in combination with agents possessing a proton exchange site can provide a significant change in the magnitude of the water proton signal, potentially providing a non-metal-based contrast mechanism [32].

When selecting a suitable CEST contrast agent, two characteristics including chemical exchange rate and longitudinal relaxation time must be considered. For maximum CEST efficiency, the chemical system must be exchanging slowly on the NMR chemical shift time-scale. A good CEST contrast agent must, therefore, possess mobile protons that exchange with water as fast as possible before exchange broadening makes selective RF presaturation ineffective. Larger frequency separations permit shorter proton lifetimes and thus result in larger CEST effects [30].

Currently, there are two major CEST contrast agents. The first CEST agents were diamagnetic small molecules (DIACEST) reported by Ward et al in 2000 [32], which contains exchangeable –NH or –OH protons. The major disadvantage of DIACEST agents is their small chemical shift difference between –NH and –OH groups and bulk water(<5ppm), which results in an overlap between the CEST effects of exogenous contrast agents and strong endogenous MT effects, and the activation of these exchange groups by semi-

selective pulses usually also results in partial saturation of bulk water protons. Another kind of CEST agents are PARACEST agents, of which chemical shift difference between two exchanging pools can be increased as much as possible. One example of PARACEST agents are Lanthanide complexes. They are stable enough for in vivo applications and have one water molecule coordinated directly to the metal ion [33], which exchanges with the bulk water molecules. The rate of water exchange is in direct relationship to the metal ion's requirement for electron density from the water molecule [33]. In more recent years, highly sensitive supramolecular and liposome-based CEST agents were developed by moving beyond the simple complex towards supramolecular structures. Two kinds of representative agents are ion-paired assemblies of poly-L-arginine and Tm^{3+}-DOTP proposed by Aime and co-workers [34] and dubbed LIPOCEST which involves the incorporation of a shift reagent, such as Tm^{3+}-DOTMA, inside a liposome [35]. To date, CEST agents present some challenges in terms of application to human studies. Although their theoretical detection limit may be lower than that of relaxation-based agents, their experimental detection limit remains higher, due to practical limitations [30].

Nowadays, there are some evdiences showing that it is possible to produce pH-sensitive MRI contrast by exploiting the exchange between the hydrogen atoms of water and the amide hydrogen atoms of endogenous mobile cellular proteins and peptides. It was reported that endogenous, low-concentration mobile proteins and peptides in tissue can be detected with amide proton transfer (APT) imaging technique via using a change in bulkwater intensity due to saturation transfer of the amide protons in the peptide bonds [36]. APT imaging is actually a variant of CEST imaging, of which the backbone is APT effect. To indicate the existence of APT effects, it was reported that there was a very small dip at frequency difference of 3.5 ppm from water, corresponding to about 8.3 ppm in the WEX spectra, where amide protons resonate [36]. Initial studies [37] have shown promise to distinguish tumor from surrounding brain in patients, but this data was hampered by magnetic field inhomogeneity and by low signal to noise ratio (SNR). Zhou [38] et al proposed a practical six-offset APT data acquisition scheme, together with a separately acquired CEST spectrum, which can provide B0-inhomogeneity corrected human brain APT images of sufficient SNR within a clinically relevant time frame.

CEST imaging, however, is also dependent on experimental parameters such as the power, duration, and waveform of the irradiation RF pulse, for which, its sensitivity and specificity for microenvironment properties such as pH is not optimal. Animal models are always used to acquire Z-spectrum, from which we can observe the offset frequency away from water resonance center, and obvious APT effect. The Z spectrum can provide good evidence for what offset frequency should be applied. However, there are still many problems about how to optimize pulse sequence for improving SNR and imaging contrast. Thus, in addition to search for better CAs, some researchers are working directly at improving pulse sequence technology. In Sun et al's study [39], they solved the dependence of CEST contrast on experimental parameters and proposed an iterative compensation algorithm that corrects the experimentally measured CEST contrast from the concomitant RF irradiation effects, thereby to accurately calibrate the chemical exchange rate.

In all, APT imaging could provide important biomarker for assessing many diseases. However, due to the low amide protons concentration (in the millimolar range), low signal-to-noise ratio, motional artifacts and so on, more efforts should be made to reach good APT imaging.

4. Measurement of pH with ^{31}P MRSI

It is reported that brain energy metabolism can be assessed by using 31P MRS to measure changes in the intracellular pH and relative concentrations of adenosinetriphosphate (ATP), phosphocreatine (PCr), and inorganic phosphate (Pi) [40-41]. By calculating from the difference in chemical shifts between Pi and PCr resonances, pH values can be obtained. As we know, although both the intracellular and extracellular compartments of tissue contain phosphate, they are different in the concentration, with 2-3 mM in intracellular compartment and 1.0 mM in extracellular compartment. Dimethyl methyl phosphate (DMMP) is a colorless liquid with chemical formula $C_3H_9O_3P$ or $CH_3PO(OCH_3)_2$. It distributed among all the water spaces. 3-aminopropylphosphonate (3-APP) has a pKa in the physiological range and accesses only the extracellular compartment. Both DMMP and 3-APP are chemically inert and non-toxic. With these materials as markers for total and extracellular water spaces respectively, non-invasively measuring the intra- and extracellular volume fraction can be accomplished [42]. For greater intracellular volume fraction and relative higher concentration of phosphate of intracellular volume, the chemical shift of the endogenous Pi resonance is generally assumed to reflect intracellular pH. Under physiological conditions, the change in intracellular pH produced by unit change in extracellular pH ranges from 0.4 to 0.8 [43-44].

In tumors, pHi of tumor cells in situ is neutral or slightly alkaline compared with that of normal tissues. Thus comparisons of intracellular pH values between systems are meaningless without knowledge of the extracellular pH [45]. Measurements of pHe in tumors have been made using an invasive microelectrodes technique. Some argument was that this invasive probe may change relative volume of cell and artifactually increase the extracellular pH. Some agents have been reported to be used as a ^{31}P-MRS indicator of extracellular pH, however, these have not also been fully developed for use in vivo [46-48]. pH indicators for in vivo use should meet some criteria which include no toxic or cytostatic effects, a pK, in the physiological range, a clearly separable signal, demonstrable localization, specificity to pH, and a large pH sensitivity [48]. An agent satisfies all these criteria is 3-APP. 3-APP is non-toxic and has a pKa in the physiological range, and in vitro results indicate that its resonant frequency is sensitive to pH and not significantly affected by temperature or ionic strength. Bioreactor experiments indicate that this compound is neither internalized nor metabolized by cells [45]. In additon, the clear separation of this signal from the cellular phosphate resonances allows extracellular pH to be measured more accurately than with extracellular Pi [45,48]. By intraperitoneally administering 3-APP , Gillies [45] et al carried out experiments in vivo which sucessfully demonstrated the use of 3-APP as a ^{31}P-MRS-based indicator of extracellular pH in cells and tissues.

5. Measruement of pH with hyperpolarized ^{13}C MRSI

^{13}C magnetic resonance spectroscopy (MRS) has long been used in the investigation of metabolic processes in vivo [49]. ^{13}C nuclear magnetic resonance (NMR) spectroscopy allows

observation of the backbone of organic compounds, yielding specific information about the identity and structure of biologically important compounds [50].With a broad chemical shift range for carbon (250ppm), which is much larger than that for proton (15 ppm), it allows for

improved resolution of metabolites. However, ^{13}C MRS is limited by the low natural abundance of ^{13}C (1.1%) and its very low nuclear spin polarization (2.5×10-6 polarization at 3 T and 37°C) [51-52].

Several techniques have been used to overcome these limitations. One way to improve the sensitivity of ^{13}C spectroscopy is to perform a technique known as proton (^{1}H) decoupling. By eliminating these couplings, the signal-to-noise ratio of ^{13}C resonances can be significantly increased via irradiating the entire ^{1}H NMR absorption range, consequently collapsing ^{13}C resonances to singlets [50]. Another technique to improve the sensitivity of ^{13}C MRS is dynamic nuclear polarization (DNP), which introduces one or more ^{13}C molecules into a metabolic substrate [53]. DNP has emerged recently as a technique for radically increasing the sensitivity of solution-state ^{13}C MRS [54]. When DNP is performed in a strong magnetic field and at cryogenic temperatures, nearly 100% nuclear polarization for ^{1}H and 50% for ^{13}C can be achieved in various organic molecules. In addition, replacing the ^{12}C isotope (98.9% natural abundance) with the ^{13}C isotope at a specific carbon or carbons in a metabolic substrate does not affect the substrate's biochemistry [52]. There are four mechanisms accounted for in the DNP process: the overhauser effect, the solid effect, thermal mixing, and the cross effect or electronuclear crosspolarization [55]. In general, the DNP experiments are conducted at low temperatures, by which to attenuate competing spin-lattice relaxation processes and avoid loss of efficiency during the polarization transfer [56]. It was reported that the sensitivity in the ^{13}C MRS experiment can be increased by 10,000-fold or more by using DNP technique, which allows not only detection of ^{13}C-labeled substrates in vivo but imaging of their tissue distribution as well [57-59]. Preclinical model clearly demonstrated the feasibility of obtaining high-spatialresolution ^{13}C MRSI data with a high signal-to-noise ratio from tumor implanted mice injected by injecting the animals with hyperpolarized 1-[^{13}C] pyruvate [59].

A new application for DNP is for measuring extracellular tissue pH using hyperpolarized ^{13}C labelled bicarbonate. Gallagher et al [60-61] generated a non-toxic, pH-probe, hyperpolarized $H^{13}CO_3^-$ and exploited the pH in tumors. With measurement of the $H^{13}CO_3^-$ and $^{13}CO_2$ concentration ratio after administration of hyperpolarized $H^{13}CO_3^-$, tissue pH could be determined by using the Henderson-Hasselbalch equation [62]:

$$pH=pKa+\log_{10}([HCO3^-]/[CO2]) \quad (1)$$

(pKa is assumed to be known in vivo)

6. Measruement of pH with ^{19}F NMR

^{19}F NMR has several distinct strengths: a large chemical shift range, high gyromagnetic ratio, no background signal from tissues inherently 12.5 times the sensitivity of ^{31}P NMR [63]. Ojugo et al [64] compare the effect of pHe measurements made by the ^{31}P probe (3-APP) with those made by the ^{19}F probe, 3-[N-(4-fluor-2-trifluoromethylphenyl)-sulphamoyl]-propionic acid (ZK-150471). Result showed, with wide chemical shift range, improved signal-to-noise and absence of signal overlap, ^{19}F pH probe ZK-150471 allowed a more rapid and precise measurement of pHe compared to 3-APP. Development of exogenous NMR pH indicators opens the opportunity to exploit ^{19}F nuclei. There were some evidences showing Fluorinated vitamin B6 derivatives have been developed for ^{19}F NMR methods to study cellular pHi and pHe. 6-FPOL (29fluoro-5- hydroxy-6-methyl-3,4-

pyridinedimethanol, 6-fluoropyridoxol) is one example. pH values are calculated from the ^{19}F spectra on the basis of chemical shift of 6-FPOL (δ_{obs}) with respect to a NaTFA (sodium trifluoroacetate) standard. Substituting (δ_{obs}) into the Henderson-Hasselbalch equation with coefficients pk_a=8.2; δ_{acid}=-9.85; δ_{base}=-19.61 and the pH is estimated [65]:

$$pH=pK_a+\log_{10}[\delta_{obs}\cdot\delta_{acid}/\delta_{base}\cdot\delta_{obs}] \quad (2)\ [66].$$

Mason et al [65] have demonstrated 6-FPOL readily enters cells and provides well resolved resonances reporting both intra- and extracellular simultaneously in whole blood), and the perfused rat heart. As mentioned above, the pKa of 6-FPOL is 8.2. It is appropriate for monitoring pH in the basic range, whereas it is not ideal for measurements under normal physiological conditions. There were some studies on modifications of vitamin B6 suggesting that the introduction of electron donating or withdrawing groups at the 4- and 5-positions of thepyridoxol ring could significantly alter the pKa of the 3-phenolic group, and the NMR properties at the 6-position [67]. He et al [68] have synthesized a series of novel fluorinated vitamin B6 analogues (6-fluoropyridoxol derivatives) as potential ^{19}F NMR pH indicators for use in vivo. The variation in chemical shift with respect to acid±base titration showed pKa values in the range 7.05±9.5 with a chemical shift sensitivity in the range 7.4±12 ppm. Among them, 6-Fluoropyridoxamine (6-FPAM) exhibits a pKa=7.05, which is closer to normal physiological pH than the parent molecule 6-FPOL (pKa=8.2), and should thus, be useful for precise and accurate measurements of pH in vivo [68].

7. Summary

Alteration in tissue pH is an indicator of many pathological processes, such as inflammation, ischaemia, renal disease, chronic lung disorders and intrauterine abnormalities and tumors. In tumors, the pH gradient exists between the intracellular (pHi) and extracellular (pHe) compartments. pHe is usually lower, and pHi could be higher or unchanging compared with normal tissue. Some evidences reaveal that cellular uptake of chemotherapeutic drugs may be depend on the pH gradient, which therefore, may help monitor tumour progression and evaluate drug treatment response. To date, pH measurement approaches have been applied with some NMR nuclei such as protons (^{1}H), phosphorus (^{31}P), fluorine (^{19}F) and carbon (^{13}C). ^{31}P-MRS has low spatial resolution (20-30ml) and is not available on standard clinical equipment, which is limited predominantly (99%) to proton (^{1}H) studies [36]. Currently, it is usually used as a control experiment when carrying ^{1}H or ^{13}C MRS study. The rapid development of contrast agents and improvement on technology attracts researchers to devote their effort on ^{1}H–MRSI for exploiting pH. As a variant of CEST imaging, APT imaging can detects endogenous, low-concentration mobile proteins and peptides in tissue using a change in bulkwater intensity due to saturation transfer of the amide protons in the peptide bonds with or without the need for exogenous contrast agents. DNP technique introduces one or more ^{13}C molecules into a metabolic substrate to improve the sensitivity of ^{13}C MRS. Based on this technology, a non-toxic, pH-probe is generated by intravenous injecting hyperpolarized $H_{13}CO_3$-. Nevertheless, the current standard clinical MRI scanners can't perform ^{13}C MRS, the addition of the ability to detect nuclei other than ^{1}H represents an added cost, and the clinical motivation to date has not been adequately demonstrated [50]. To date, due to the low amide protons concentration (in the millimolar range), low signal-to-noise ratio, motional artifacts and so on, to reach a good APT imaging may require long stage of development.

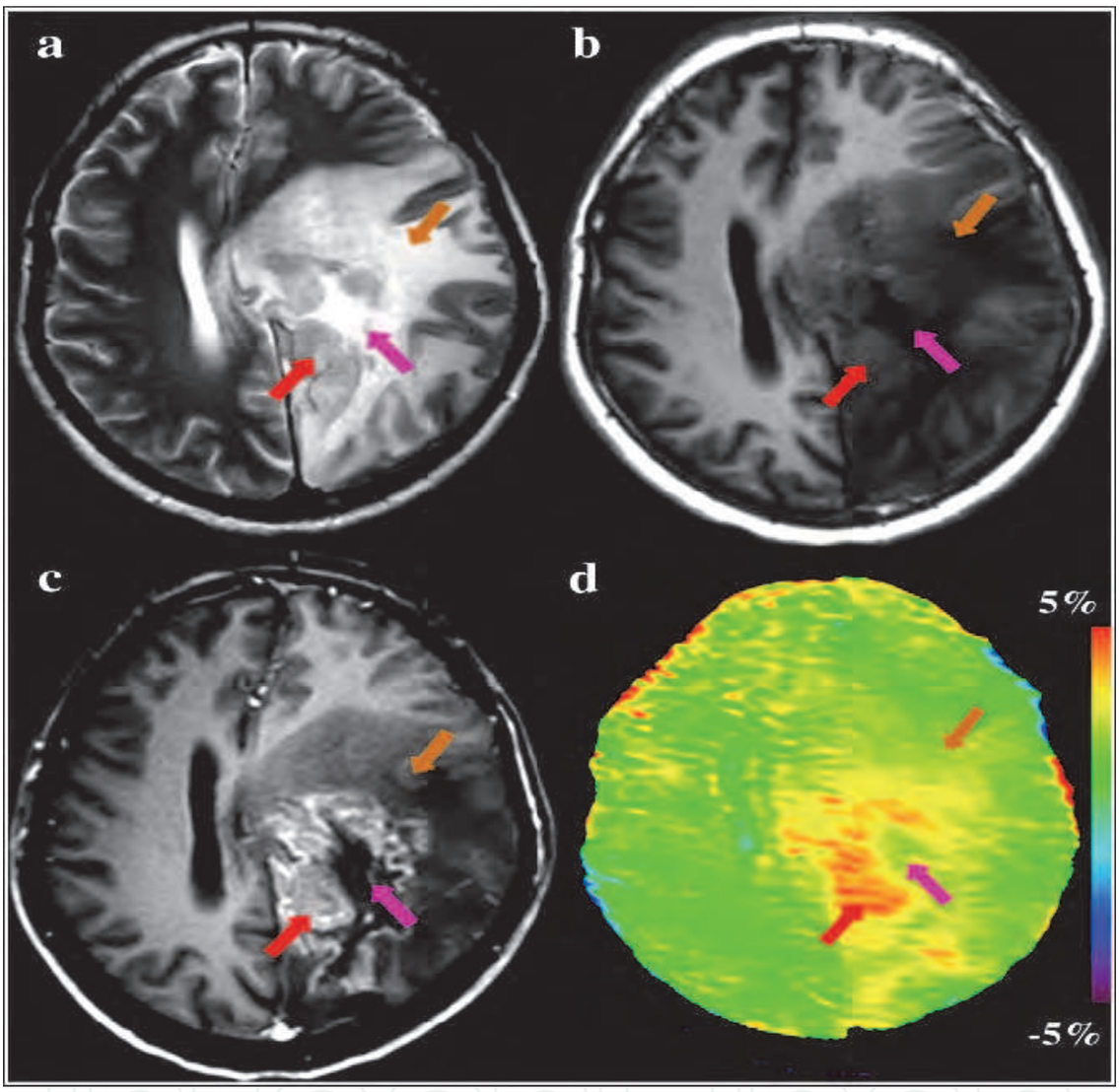

(Courtesy of Dr Jinyuan Zhou and Elsevier)

Fig. 1. MR images acquired on a Philips 3 T MRI scanner (Achieva 3.0 T; Philips Medical Systems, Best, The Netherlands) from a patient with recurrent astrocytoma (grade III), acquired four months after treatment. (a), (b) T2-weighted image and T1-weighted image show the recurrence of glioma with heterogeneous intensity in the left parietal lobe. The exact location of the tumor core is obscure. (c) Post-contrast T1-weighted image reveals a gadolinium-enhancing tumor core (red arrow) and a necrotic area (pink arrow). The recurrent tumor is associated with the surrounding edema and mass effect. (d) APT image shows an obvious increase in APT signal intensity in the tumor core. The regions of necrosis (pink arrow) and edema (orange arrow) are almost isointense on APT.

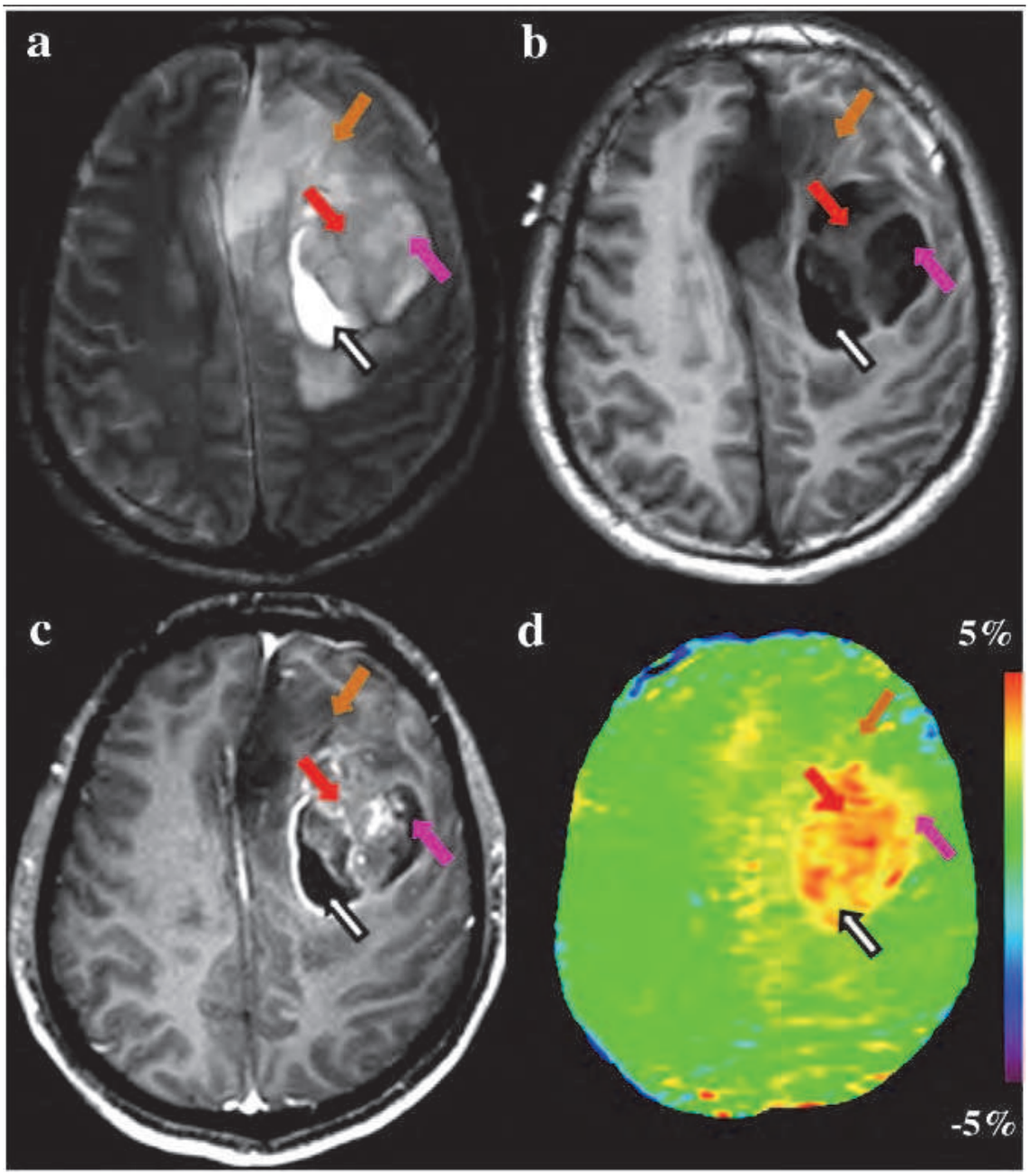

(Courtesy of Dr Jinyuan Zhou and Elsevier)

Fig. 2. MR images for another patient with glioblastoma multiforme. (a), (b) T2-weighted image T1-weighted image show a large tumor of abnormal signals in the left frontal lobe. (c) Gadolinium-enhanced T1-weighted image demonstrates an enhancing tumor core (red arrow) with non-enhancing necrotic areas. (d) APT image shows that both the gadolinium-enhancing tumor core (red arrow) and the cystic cavity (black arrow) have high APT signal intensities, while the necrotic regions (pink arrow) and edema areas (orange arrow) have low APT signal intensities.

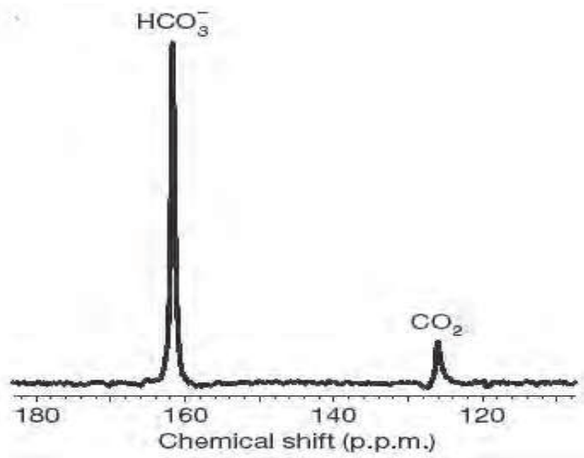

(Courtesy of Dr Kevin M. Brindle)

Fig. 3. 13C spectrum from a murine lymphoma (EL4) tumour in vivo, acquired 10 s after the intravenous injection of hyperpolarized H13CO3-, showing resonances from H13CO3- (at 161 p.p.m.) and 13CO2 (at 125 p.p.m.).

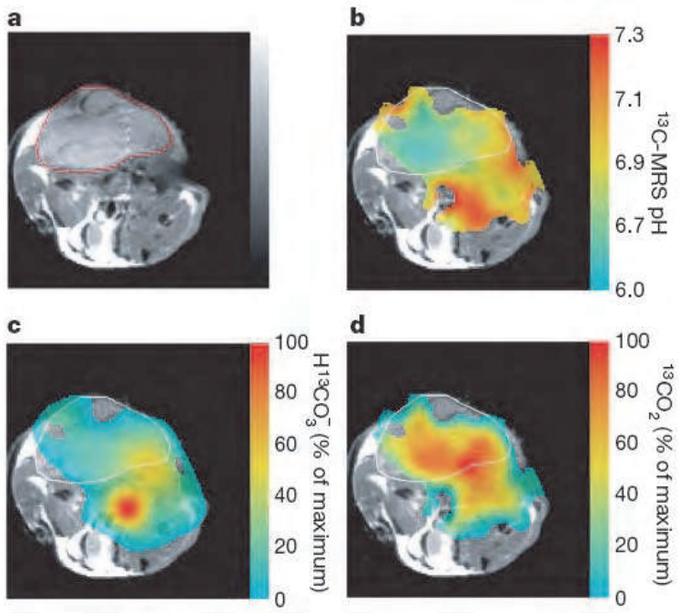

(Courtesy of Dr Kevin M. Brindle)

Fig. 4. The spatial distribution of 13CO2 and H13CO3- in a transverse slice was imaged using a gradient echo pulse sequence. A shows transverse proton magnetic resonance image of a mouse with a subcutaneously implanted EL4 tumour. Tumor is margined in red. B shows the pH map calculated from the ratio of the H13CO3- and 13CO2 voxel intensities ,which demonstrated a low intratumoral pH. C and d show the spatial distribution of H13CO3- and 13CO2, displayed as voxel intensities relative to their respective maxima, respectively. the highest concentration of 13CO2 was in the tumour and the H13CO3- signal was highest in the aorta and there was little difference in signal intensities between muscle and tumour. The tumour margin in b, c and d is outlined in white.

(Courtesy of Dr Ralph Mason)

Fig. 5. Struture of 6-FPOL(6-fluoropyridoxol)

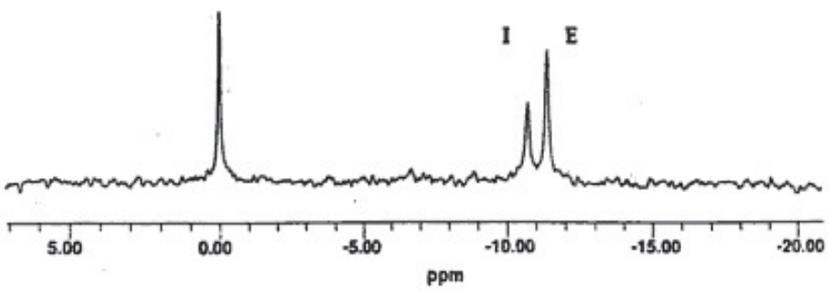

a

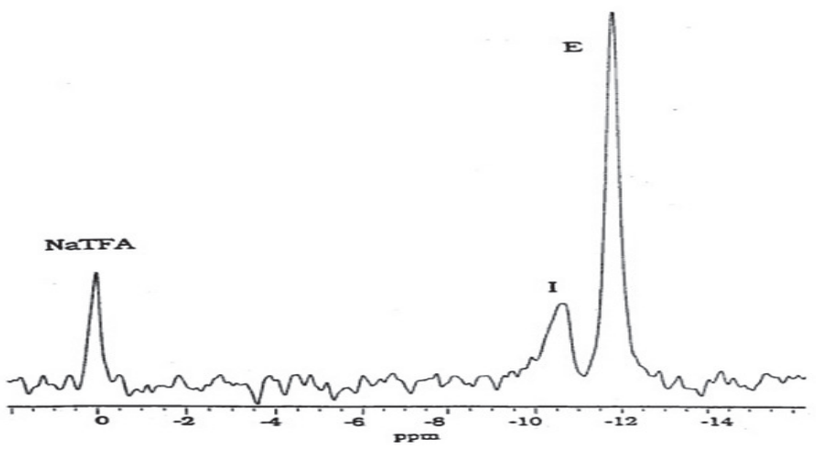

B

(Courtesy of Dr Ralph Mason)

Fig. 6. a 282MHz 19F NMR spectrum of 6-FPOL in whole unwashed rabbit blood:pHi=7.19(δ=-10.72ppm).pHe 7.45(δ=-11.34ppm). ΔpH=0.26(Δδ=0.62ppm) with respect to external NaTFA capillary standard. 6b 376MHz 19F NMR spectrum of 6-FPOL in a sanguinous perfused rat heart: pHi=7.16(δ=-10.60ppm).pHe 7.55(δ=-11.64ppm). ΔpH=0.39(Δδ=1.04ppm) with respect to external NaTFA in balloon in left ventricle.

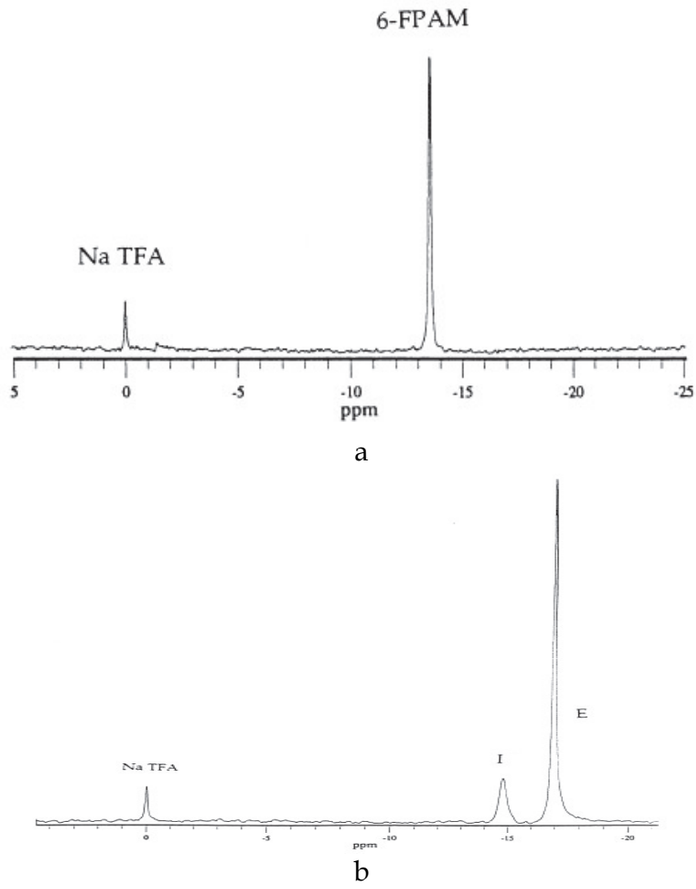

(Courtesy of Sha He and Elsevier)

Fig. 7. a 19F NMR spectrum of 6-FPAM in water at pH 6.9 (δ=-13.57 ppm). 7b Spectrum of 6-FPAM in whole rabbit blood. Two signals are observed for 6-FPAM attributed to intra (δ=-14.793 ppm) and extra (δ=-16.935 ppm) cellular compartments corresponding to pH 7.16 and 7.59, respectively. A capillary of sodium TFA served as external chemical shift reference.

8. References

[1] Gillies RJ, Raghunand N, Garcia-Martin ML, Gatenby RA. pH imaging. A review of pH measurement methods and applications in cancers. IEEE Eng Med Biol Mag. 2004; 23(5):57-64.

[2] Adrogue HJ, Madias NE. Management of life-threatening acid-base disorders. First of two parts. N. Engl. J. Med.1998, 338, 26–34

[3] Hohn-Berlage M, Okada Y, Kloiber O , Hossmann KA. Imaging of brain tissue pH and metabolites. A new approach for the validation of volume-selective NMR spectroscopy. NMR Biomed. 1989, 2, 240–245.

[4] Grinstein S, Swallow CJ, Rotstein OD. Regulation of cytoplasmic pH in phagocytic cell function and dysfunction. Clin. Biochem. 1991, 24, 241–247.

[5] Gerweck LE, Seetharaman K. Cellular pH gradient in tumor versus normal tissue: potential exploitation for the treatment of cancer. Cancer Res. 1996; 56(6):1194-8.
[6] Wike-Hooley JL, Haveman J, Reinhold HS. The relevance of tumour pH to the treatment of malignant disease. Radiother. Oncol, 1984, 2: 343-366,
[7] Gulledge CJ, Dewhirst MW. Tumor oxygenation: a matter of supply and demand. Anticancer Res, 1996, 16: 741–750.
[8] Prescott DM, Charles HC, Poulson JM, Page RL, Thrall DE, Vujaskovic Z, Dewhirst MW. The relationship between intracellular and extracellular pH in spontaneous canine tumors. Clin Cancer Res. 2000; 6(6):2501-5.
[9] Engin K, Leeper DB, Cater JR, Thistlethwaite AJ, Tupchong L, McFarlane JD. Extracellular pH distribution in human tumours. Int. J. Hyperthermia, 1995, 11: 211–216.
[10] Vaupel P, Kallinowski F, Okunieff P. Blood flow, oxygen and nutrient supply, and metabolic microenvironment of human tumors: a review. Cancer Res. 1989, 49:6449–6465,.
[11] Robert JRK, Wade-Jardetzsky N, Jardetzsky O. Intracellular pH measurements by ^{31}P-NMR. Influence of factors other than pH on f/P chemical shifts. Biochemistry. 1981, 20: 5389-5392.
[12] Gerweck LE, Vijayappa S, Kozin S. Tumor pH controls the in vivo efficacy of weak acid and base chemotherapeutics. Cancer Res.1996, 56: 1194–1198.
[13] Simon S, Roy D, and Schindler M. Intracellular pH and the control of multidrug resistance. Proc. Natl. Acad. Sci. USA, 1994, 91: 1128– 1132.
[14] Kozin SV, Shkarin P, Gerweck LE. The cell transmembrane pH gradient in tumors enhances cytotoxicity of specific weak acid chemotherapeutics. Cancer Res. 200; 61(12):4740-3.
[15] Atema A, Buurman KJ, Noteboom E, and Smets LA. Potentiation of DNA-adduct formation and cytotoxicity of platinumcontaining drugs by low pH. Int. J. Cancer, 1993, 54: 166–172.
[16]Vukovic V, Tannock IF. Influence of low pH on cytotoxicity of paclitaxel, mitoxantrone and topotecan. Br. J. Cancer, 1997, 75: 1167– 1172.
[17] Engin K, Leeper DB, ThistlethwaiteAJ, Tupchong L, McFarlane JD. Tumor extracellular pH as a prognostic factor in thermoradiotherapy. Int. J. Radiat. Oncol. Biol. Phys., 29: 125–132, 1994.
[18] Song, CW, Lyons JC, Luo Y. Intra- and extracellular pH in solid tumors: Influence on therapeutic response. In Drug Resistance in Oncology, B Teicher (ed), 1993b, pp. 25–51. Marcel Dekker: New York
[19] Newell KJ, Tannock IF. Reduction of intracellular pH as a possible mechanism for killing cells in acidic regions of solid tumors: effects of carbonylcyanide-3-chlorophenylhydrazone. Cancer Res. 1989, 49: 4477-4482.
[20] Evelhoch JL. pH and therapy of human cancers. Novartis Found Symp. 2001; 240:68-80.
[21] van Sluis R, Bhujwalla ZM, Raghunand N, Ballesteros P, Alvarez J, Cerdán S, Galons JP, Gillies RJ. In vivo imaging of extracellular pH using1H-MRSI, Magn Reson Med. 1999; 41(4):743-50 .
[22] Qiu QC,Wei MB,Shen ZW, Wu RH.T2-weighted magnetic resonance imaging based on the different pH values. Chinese Journal of Medical Physics, 2009, 26(5):1405-08.

[23] Hartman KB, Laus S, Bolskar RD, Muthupillai R, Helm L, Toth E, Merbach AE, Wilson LJ. Gadonanotubes as ultrasensitive pH-smart probes for magnetic resonance imaging. Nano Lett. 2008; 8(2):415-9.

[24] Broome DR. Nephrogenic systemic fibrosis associated with gadolinium based contrast agents: a summary of the medical literature reporting. Eur. J. Radiol. 2008, 66, 230–234.

[25] Woods M, Kiefer GE, Bott S, Castillo-Muzquiz A, Eshelbrenner C, Michaudet L, McMillan K, Mudigunda SD, Ogrin D, Tircsó G, Zhang S, Zhao P, Sherry AD. Synthesis, relaxometric and photophysical properties of a new pH-responsive MRI contrast agent: the effect of other ligating groups on dissociation of a p-nitrophenolic pendant arm. J Am Chem Soc. 2004; 126(30):9248-56.

[26] Zhang S, Wu K, Sherry AD. Gd3+ complexes with slowly exchanging bound-water molecules may offer advantages in the design of responsive MR agents. Invest Radiol. 2001; 36(2):82-6.

[27] Jebasingh B, Alexander V. Synthesis and relaxivity studies of a tetranuclear gadolinium(III) complex of DO3A as a contrast-enhancing agent for MRI. Inorg Chem. 2005; 44(25):9434-43.

[28] Lowe MP, Parker D, Reany O, Aime S, Botta M, Castellano G, Gianolio E, Pagliarin R. pH-dependent modulation of relaxivity and luminescence in macrocyclic gadolinium and europium complexes based on reversible intramolecular sulfonamide ligation. J Am Chem Soc. 2001; 123(31):7601-9.

[29] Sitharaman B, Wilson LJ. Gadonanotubes as new high-performance MRI contrast agents. Int J Nanomedicine. 2006; 1(3):291-5. protons.

[30] Hancu I, Dixon WT, Woods M, Vinogradov E, Sherry AD, Lenkinski RE. CEST and PARACEST MR contrast agents. Acta Radiol. 2010; 51(8):910-23.

[31] Huinink HP, Sanders HM, Erich SJ, Nicolay K, Strijkers GJ, Merkx M, et al. High-resolution NMR imaging of paramagnetic liposomes targeted to a functionalized surface. Magn Reson Med 2008; 59:1282–6

[32] Ward KM, Aletras AH, Balaban RS. A new class of contrast agents for MRI based on proton chemical exchange dependent saturation transfer (CEST). J Magn Reson 2000; 143:79–87.

[33] Merbach AE, Toth E, editors. The chemistry of contrast agents in medical magnetic resonance imaging. New York: Wiley; 2001.

[34] Aime S, Delli Castelli D, Terreno E. Supramolecular adducts between poly-L-arginine and [TmIIIdotp]: a route to sensitivity- enhanced magnetic resonance imaging-chemical exchange saturation transfer agents. Angew Chem Int Ed Engl 2003; 42:4527–9

[35] Aime S, Delli Castelli D, Terreno E. Highly sensitive MRI chemical exchange saturation transfer agents using liposomes. Angew Chem Int Ed Engl 2005; 44:5513–15.

[36] Zhou J, Payen JF, Wilson DA, Traystman RJ, van Zijl PC. Using the amide proton signals of intracellular proteins and peptides to detect pH effects in MRI. Nat Med. 2003; 9(8):1085-90.

[37] Wen Z, Hu S, Huang F, Wang X, Guo L, Quan X, Wang S, Zhou J. MR imaging of high-grade brain tumors using endogenous protein and peptide-based contrast.
Neuroimage. 2010; 51(2):616-22.

[38] Zhou J, Blakeley JO, Hua J, Kim M, Laterra J, Pomper MG, van Zijl PC. Practical data acquisition method for human brain tumor amide proton transfer (APT) imaging. Magn Reson Med. 2008; 60(4):842-9.

[39] Sun PZ, Sorensen AG.Imaging pH using the chemical exchange saturation transfer (CEST) MRI: Correction of concomitant RF irradiation effects to quantify CEST MRI for chemical exchange rate and pH. Magn Reson Med. 2008; 60(2):390-7.

[40] Wu RH, Poublanc J, Mandell D, et al. Evidence of brain mitochondrial activities after oxygen inhalation by 31P magnetic resonance spectroscopy at 3T. Conf Proc IEEE Eng Med Biol Soc, 2007, pp. 2899-2902.

[41] Wu RH, Liu WW, Chen YW, Wang H, Shen ZHW, Brugge KT and Mikulis DJ. Preliminary study of mapping brain ATP and brain pH using multivoxel ^{31}P MR spectroscopy. 13th International Conference on Biomedical Engineering IFMBE Proceedings, 2009, Volume 23, Track 1, 362-365, DOI: 10.1007/978-3-540-92841-6_89.

[42] Bhujwalla ZM, McCoy CL, Glickson JD, Gillies RJ, Stubbs M. Estimations of intra- and extracellular volume and pH by ^{31}P magnetic resonance spectroscopy: effect of therapy on RIF-1 tumours. Br J Cancer. 1998; 78(5):606-11

[43] Gillies RJ. Intracellular pH and growth control in eukaryoticcells. In: The Transformed Cell, edited by I. L. Cameron and T. B. Poole. New York: Academic, 1981, p. 347-395.

[44] Wilding T J, Boron W. pH regulation in adult rat carotid body glomus cells: importance of extracellular pH, sodium, and potassium. J. Gen. Physiol. 1992, 100: 593-608.

[45] Gillies RJ, Liu Z, Bhujwalla Z. ^{31}P-MRS measurements of extracellular pH of tumors using 3-aminopropylphosphonate. Am J Physiol. 1994; 267(1 Pt 1):C195-203.

[46] Fisher MJ, Dillon PF. Phenylphosphate: a ^{31}P-NMR indicator of extracellular pH and volume in the isolated perfused rabbit bladder. Circ. Res. 1987, 60: 472-477.

[47] Meyer R A, Brown TR, Kusmerick MJ. Phosphorus nuclear magnetic resonance of fast- and slow-twitch muscle. Am. J. Physiol. 1985, 248 (CeZZ Physiol. 17): C279-C287.

[48] Szwergold BS. NMR spectroscopy of cells. Annu. Rev. Physiol. 1992, 54:775-798,.

[49] Shulman RG, Brown TR, Ugurbil K, Ogawa S, Cohen SM and den Hollander JA. Cellular applications of ^{31}P and ^{13}C nuclear magnetic resonance. Science 1979, 205, 160–166

[50] Kurhanewicz J, Bok R, Nelson SJ, Vigneron DB. Current and potential applications of clinical 13C MR spectroscopy. J Nucl Med. 2008; 49(3):341-4.

[51] Rajesh A, Coakley FV, Kurhanewicz J. 3D MR spectroscopic imaging in the evaluation of prostate cancer. Clin Radiol 2007;62:921–929.

[52] Shan L. Hyperpolarized 13C-labeled bicarbonate (H13CO3 -) for in vivo pH measurement with 13C magnetic resonance spectroscopy. Molecular Imaging and Contrast Agent Database (MICAD) [Internet]. Bethesda (MD): National Center for Biotechnology Information (US); 2004-2010.

[53] Golman K, Olsson LE, Axelsson O, Mansson S, Karlsson M, Petersson JS. Molecular imaging using hyperpolarized ^{13}C. Br J Radiol 2003; 76 (Spec No 2):S118–27.

[54] Ardenkjaer-Larsen JH et al. Increase in signal-to-noise ratio of 10,000 times in liquid-state NMR. Proc. Natl Acad. Sci. USA 2003, 100, 10158–10163.

[55] Joo CG, Hu KN, Bryant JA. Griffin RG. In situ temperature jump high-frequency dynamic nuclear polarization experiments: enhanced sensitivity in liquid-state NMR spectroscopy. J Am Chem Soc 2006; 128(29):9428–32.

[56] Zhang H. Hyperpolarized sodium 1-[13C]pyruvate. Molecular Imaging and Contrast Agent Database (MICAD) [Internet]. Bethesda (MD): National Center for Biotechnology Information (US); 2004-2010.

[57] Golman K, Ardenkjaer-Larsen JH, Petersson JS, Mansson S, Leunbach I.Molecular imaging with endogenous substances. Proc. Natl. Acad. Sci. USA 2003, 100, 10435–10439.

[58] Golman K, Petersson, JS. Metabolic imaging and other applications of hyperpolarized 13C. Acad. Radiol. 2006, 13, 932–942.

[59] Golman K, Zandt RI, Lerche M, Pehrson R, Ardenkjaer-Larsen JH. Metabolic imaging by hyperpolarized 13C magnetic resonance imaging for in vivo tumor diagnosis. Cancer Res. 2006, 66, 10855–10860.

[60] Gallagher FA, Kettunen MI, Day SE, Hu DE, Ardenkjaer-Larsen JH, Zandt R, Jensen PR, Karlsson M, Golman K, Lerche MH, Brindle KM. Magnetic resonance imaging of pH in vivo using hyperpolarized 13C-labelled bicarbonate. Nature. 2008; 453(7197):940-3.

[61] Day SE, Kettunen MI, Gallagher FA, Hu DE, Lerche M, Wolber J, Golman K, Ardenkjaer-Larsen JH, Brindle KM. Detecting tumor response to treatment using hyperpolarized 13C magnetic resonance imaging and spectroscopy. Nat Med. 2007; 13(11):1382-7.

[62] White A, Handler P, Smith EL. Principles of Biochemistry (McGraw-Hill Kogakusha, New York, 1968). Stabenau EK, Heming TA. Determination of the constants of the

Henderson- Hasselbalch equation, aCO2 and pKa, in sea turtle plasma. J. Exp. Biol. 1993, 180, 311–314.

[63] Gadian DG. NMR and its application to living systems; 2nd ed; OUP: Oxford,1995

[64] Ojugo AS, McSheehy PM, McIntyre DJ, McCoy C, Stubbs M, Leach MO, Judson IR, Griffiths JR. Measurement of the extracellular pH of solid tumours in mice by magnetic resonance spectroscopy: a comparison of exogenous (19) F and (31)P probes. NMR Biomed. 1999; 12(8):495-504.

[65] Mason RP. Transmembrane pH gradients in vivo: measurements using fluorinated vitamin B6 derivatives. Curr Med Chem. 1999; 6(6):481-99.

[66] Roos A, Boron WF. Intracellular pH. Physiol Rev 1981; 61:296-434

[67] Scott RD, Chang YC, Graves DJ, Metzler DE. Studies of 6-fluoropyridoxal and 6-fluoropyridoxamine 5′-phosphate in cytosolic aspartate aminotransferase. Biochemistry 1985, 24, 7668-7681

[68] He S, Mason RP, Hunjan S, Mehta VD, Arora V, Katipally R, Kulkarni PV, Antich PP. Development of novel 19F NMR pH indicators: synthesis and evaluation of a series of fluorinated vitamin B6 analogues. Bioorg Med Chem.1998; 6(9):1631-9.

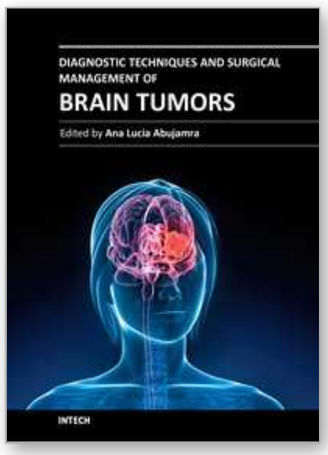

Diagnostic Techniques and Surgical Management of Brain Tumors
Edited by Dr. Ana Lucia Abujamra

ISBN 978-953-307-589-1
Hard cover, 544 pages
Publisher InTech
Published online 22, September, 2011
Published in print edition September, 2011

The focus of the book Diagnostic Techniques and Surgical Management of Brain Tumors is on describing the established and newly-arising techniques to diagnose central nervous system tumors, with a special focus on neuroimaging, followed by a discussion on the neurosurgical guidelines and techniques to manage and treat this disease. Each chapter in the Diagnostic Techniques and Surgical Management of Brain Tumors is authored by international experts with extensive experience in the areas covered.

INTECH
open science | open minds

InTech Europe
University Campus STeP Ri
Slavka Krautzeka 83/A
51000 Rijeka, Croatia
Phone: +385 (51) 770 447
Fax: +385 (51) 686 166
www.intechopen.com

InTech China
Unit 405, Office Block, Hotel Equatorial Shanghai
No.65, Yan An Road (West), Shanghai, 200040, China
中国上海市延安西路65号上海国际贵都大饭店办公楼405单元
Phone: +86-21-62489820
Fax: +86-21-62489821

IntechOpen